



Steady-state Visual Evoked Potentials Reveal Dynamic (Re)allocation of Spatial Attention during Maintenance and Utilization of Visual Working Memory

Samson Chota^{ID}, Arnaud T. Bruat, Stefan Van der Stigchel, and Christoph Strauch

Abstract

■ Visual working memory (VWM) allows storing goal-relevant information to guide future behavior. Prior work suggests that VWM is spatially organized and relies on spatial attention directed toward locations at which memory items were encoded, even if location is task-irrelevant. Importantly, attention often needs to be dynamically redistributed between locations, for example, in preparation for an upcoming probe. Very little is known about how attentional resources are distributed between multiple locations during a VWM task and even less about the dynamic changes governing such attentional shifts over time. This is largely due to the inability to use behavioral outcomes to reveal fast dynamic changes within trials. We here demonstrated that EEG steady-state visual evoked potentials (SSVEPs) successfully track the dynamic allocation of spatial attention during a VWM task. Participants were presented with to-be-memorized gratings and distractors at two distinct locations, tagged with flickering discs. This allowed us to dynamically track attention

allocated to memory and distractor items via their coupling with space by quantifying the amplitude and coherence of SSVEP responses in the EEG signal to flickering stimuli at the former memory and distractor locations. SSVEP responses did not differ between memory and distractor locations during early maintenance. However, shortly before probe comparison, we observed a decrease in SSVEP coherence over distractor locations indicative of a reallocation of spatial attentional resources. RTs were shorter when preceded by stronger decreases in SSVEP coherence at distractor locations, likely reflecting attentional shifts from the distractor to the probe or memory location. We demonstrate that SSVEPs can inform about dynamic processes in VWM, even if location does not have to be reported by participants. This finding not only supports the notion of a spatially organized VWM but also reveals that SSVEPs betray a dynamic prioritization process of working memory items and locations over time that is directly predictive of memory performance. ■

INTRODUCTION

Visual working memory (VWM) allows for temporarily storing information such as the appearance and location of objects that are presumed relevant for future behavior (Baddeley, 1992; Logie & Marchetti, 1991). Although attention is an essential component of VWM, little is known about how its spatial allocation changes over time during maintenance and utilization of memoranda (Awh, Vogel, & Oh, 2006). Past work has highlighted that working memory is spatially grounded by demonstrating that spatial attention is automatically biased toward memorized locations (Awh & Jonides, 2001). Spatial attention and working memory likely share neural mechanisms, as drawing spatial attention away from memorized locations results in impaired reports (Awh & Jonides, 2001; Awh, Jonides, & Reuter-Lorenz, 1998; Smyth, 1996).

Intriguingly, memory location-specific effects on attention can also be observed “when the location itself is irrelevant,” for example, when only the color, but not the location, of an item needs to be reported (Theeuwes,

Kramer, & Irwin, 2011; but see also Awh et al., 1998). So far, these effects have been studied with so-called retro-cues—cues that direct attention to memoranda after templates have been taken away. Retro-cued items are associated with better recall performance (Souza & Oberauer, 2016). In a recent series of experiments, participants were tasked with memorizing the orientation of two colored bars presented in the periphery, after which color retro-cues at fixation indicated which item would likely be subsequently probed (van Ede, Deden, & Nobre, 2021; van Ede, Board, & Nobre, 2020; van Ede, Chekroud, & Nobre, 2019). Results showed that retro-cues led to gaze biases toward the location of cued items, even though that location did not have to be remembered nor did the memory probe ever appear in that location. Such directional biases in gaze can track the direction of covert spatial attention (Zhou & Desimone, 2011; Engbert & Kliegl, 2003; Kustov & Lee Robinson, 1996; Schall & Hanes, 1993) and are assumed to index attentional selection within working memory. Location is therefore likely an essential component of VWM representations with location taking a grounding role in VWM

storage (van Ede et al., 2019; Schneegans & Bays, 2017). This conclusion is further supported by electrophysiological evidence demonstrating that markers of attentional selection such as alpha lateralization (Liu, Nobre, & van Ede, 2022, 2023; Foster, Bsaies, Jaffe, & Awh, 2017; Poch, Capilla, Hinojosa, & Campo, 2017; van Ede, Niklaus, & Nobre, 2017; Poch, Campo, & Barnes, 2014) and the N2Pc ERP (Dell'Acqua, Sessa, Toffanin, Luria, & Jolicœur, 2010; Kuo, Rao, Lepsien, & Nobre, 2009) as well as markers of VWM storage such as contralateral delay activity (Eimer & Kiss, 2010) show similar spatial biases. We here extend this toolbox by utilizing SSVEPs as a continuous item-specific measure of spatial attention.

It is becoming increasingly evident that VWM needs to be viewed as a dynamic and flexible process reflecting the fast changing environment in which it is utilized (Nobre & van Ede, 2023; Buschman & Miller, 2022; Chota & Van der Stigchel, 2021). Novel methods capable of capturing fast changes in the prioritization of memoranda as well as their interaction with the external world are therefore urgently needed. We therefore set out to test whether steady-state visual evoked potentials (SSVEPs) allow to study spatio-temporal dynamics of latent “internal” attention in VWM. Our approach is inspired by previous findings, suggesting that during VWM maintenance spatial attention is distributed among memory items. We hypothesized that this might result in location-specific enhancements in perceptual processing that can be measured using SSVEPs. Furthermore we sought to investigate how attentional resources are “spatially” distributed between multiple relevant or irrelevant locations during a VWM task. This question has proven difficult to answer using classical methods of measuring covert attention such as microsaccades. For instance, it was recently demonstrated that microsaccades are directed toward the midpoint between two items, irrespective of one or both being cued as behaviorally relevant (Willett & Mayo, 2023), showing a limitation of spatial specificity of microsaccades in some cases. Furthermore, prior behavioral studies utilized dual tasks during the maintenance period to probe spatial attention, which could be a potentially confounding factor as these tasks themselves require allocation of spatial attention to memory locations, for example, to detect a target (Golomb, Chun, & Mazer, 2008; Awh & Jonides, 2001). Last, we were interested in quantifying the temporal profile of this hypothesized spatial distribution of attention. More specifically, how is spatial attention (re)allocated between memory, distractor, or probe locations in the course of a trial?

We used EEG SSVEPs, rhythmic brain responses to flickering stimuli, that have been shown to increase in amplitude and phase consistency as a result of covert attention allocated to the flickering stimulus location (Gulbinaite, Roozendaal, & VanRullen, 2019; Gulbinaite, van Viegen, Wieling, Cohen, & VanRullen, 2017; Kashiwase, Matsumiya, Kuriki, & Shioiri, 2012; Walter, Quigley, Andersen, & Mueller, 2012; Andersen, Müller, & Hillyard, 2009; Müller et al., 2006; Morgan, Hansen, & Hillyard,

1996). They allow for direct and highly time-resolved measures of spatial attention and ensuing facilitation of sensory processing, without the need for a secondary behavioral task. In the current experiment, participants were presented with two tilted gratings at distinct spatial locations. Participants were instructed to memorize the identity but not location of both (memory + memory) or only one (memory + distractor) grating. We subsequently presented two flickering discs over both locations, which allowed us to measure the magnitude of SSVEP responses (spatial attention) allocated to memory and distractor locations during maintenance and preparation for probe comparison. This enabled us to compare how attention was dynamically allocated between one or two locations previously occupied by memory items or distractors.

We showcase that SSVEP responses are a powerful new approach to quantify dynamic changes in internal attention toward individual items in working memory. We found enhanced SSVEP responses at memory compared with distractor locations, supporting the notion of a spatially organized and spatially selective VWM. Crucially, time-resolved analysis of SSVEP responses showed a decrease in attention directed toward distractor locations shortly before probe presentation, indicating a reallocation of attention toward the upcoming central probe location. This decrease did not occur for memory locations and predicted subsequent RTs: Participants with a relatively stronger attentional reallocation/suppression of the distractor location tended to respond faster to probes. This shows that the flexible use of limited attentional resources during VWM is key for efficient task performance. Furthermore, we found that SSVEP responses were not reduced when attention was distributed between two memory locations as compared with one, potentially because in the latter attentional resources were distributed equally between memory and distractor locations before being reallocated shortly before probe presentation. Our findings confirm accounts of a spatial organization of VWM and demonstrate that VWM maintenance and utilization is accompanied by dynamic, location-specific, and behaviorally relevant (re)distribution of spatial attention.

METHODS

Participants

Twenty-six participants (14 female, 12 male) with normal or corrected-to-normal vision enrolled in the experiment. Our sample size was chosen to provide similar or better statistical power than comparable SSVEP studies (Andersen et al., 2009, $n = 17$; Toffanin, de Jong, Johnson, & Martens, 2009, $n = 14$). None of the participants reported a history of psychiatric or neurological diagnosis such as photic epilepsy. Informed consent forms were signed before the experiment. The study was carried out in accordance with the protocol approved by the ethics committee of the Faculty of Social and Behavioral Sciences of

Utrecht University and followed the Code of Ethics of the World Medical Association (Declaration of Helsinki). Participants were compensated with 10 €/hr.

Stimuli

Memory and probe stimuli consisted of black and white oriented gratings (diameter: 4° dva, spatial frequency: 4 cpdva) whose orientation was randomly selected on every trial (12°, 42°, 72°, 102°, 132°, 162°). Memory orientations in the two-item condition were always distinct. Distractors used in the one-item condition were created using a Mondrian mask (diameter: 4° dva, code from Christophel, Hebart, & Haynes, 2012). A large rectangular mask using the identical Mondrian pattern was presented centrally following the memory and distractor items to prevent afterimages (height: 5° dva, width: 8° dva). SSVEP stimuli consisted of circular discs (diameter: 4° dva) and were sinusoidally modulated at a frequency of 10 and 13.333 Hz. These frequencies were chosen to allow for a precise estimation of their power within a 1.5-sec window.

Protocol

Stimuli were presented on an LED monitor (Asus RoG Swift PG278Q, 27-in., 2560 × 1440 resolution, 120 Hz refresh rate, black–white–black RT 8.6 msec, gray–gray RT 6.9 msec) using the Psychophysics Toolbox (Kleiner et al., 2007; Brainard, 1997) running in MATLAB

(The MathWorks). Participants were seated 58 cm from the screen on a chinrest to prevent excessive head movements.

Participants performed a delayed match-to-sample task, in which they reported whether the orientation of the probe matched either of the initially memorized stimuli. At the beginning of each block, participants were informed about the number of items they were required to memorize in this particular block (“one-item condition” vs. “two-item condition”). The starting block of individual participants was randomized, and item conditions alternated between blocks. Each block contained 44 trials, and participants performed a total of 14 blocks (2 training blocks, 88 trials total + 12 experimental blocks, 528 trials total).

Trials began with a central black fixation cross presented for 1500 msec on gray background. A sequence of two items (one-item condition: distractor + memory, two-item condition: Memory A + Memory B) was presented to the left and right side of fixation in a randomized order (eccentricity: 4° dva; Figure 1). The first item was presented for a random duration between 200 and 500 msec (steps of 30 msec), followed by the second item which was presented for a duration of 100 msec. The presentation time of the first item was varied to prevent participants from developing precise temporal expectations for the onset of the second stimulus. The temporal order and position of memory and distractor presentation was randomized. After a screen containing only the fixation cross (200 msec), a large rectangular mask (500 msec) was

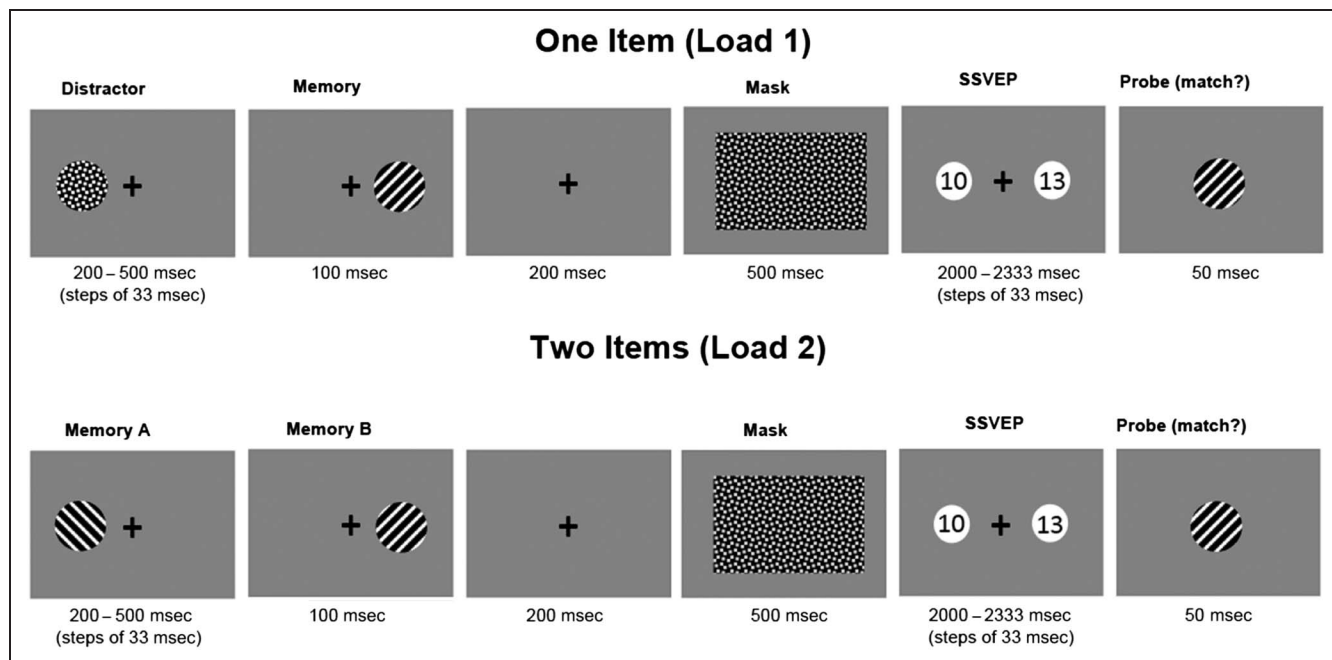


Figure 1. Participants performed a delayed match-to-sample task. In the one-item (Load 1), condition participants were presented with one to-be-memorized oriented grating and one distractor in random order and at a random location left or right of fixation. The two-item condition was identical to the one-item condition, except that a second to-be-memorized memory item was presented instead of a distractor. Stimulus presentation was followed by a mask, and subsequently, two flickering discs were presented at the same location at which the initial stimuli were presented. Probes were presented at fixation, and participants indicated whether the probes’ orientation matched either of the initial memory items.

presented to prevent afterimage effects on the SSVEP responses. This mask was immediately followed by two circular SSVEP entrainers whose position overlapped with the original location of the memory items and/or distractors. The SSVEP stimuli flickered for a variable delay of 2000 to 2330 msec (in steps of 30 msec) with 13.333 Hz always being presented on the right and 10 Hz always being presented on the left side. SSVEP duration was varied to prevent participants from developing precise temporal expectations on the appearance of the probe. The location of the flicker frequencies was kept identical throughout the task to allow for the inclusion of all trials in the rhythmic entrainment source separation (RESS) procedure, which significantly increases the signal-to-noise ratio (SNR) for the construction of the spatial filters (see SSVEP and RESS under Methods section). Subsequently, the probe was centrally presented for 50 msec, either matching the orientation of one of the initially presented items (75%) or matching none of the items (25%). In the case of a nonmatch, its orientation was randomly drawn from one of the remaining orientations not used for a sample. Participants were given 1500 msec to report either a match (keyboard button P) or a mismatch (keyboard button Q) after which they received feedback. Feedback was presented in the form of the fixation cross turning green (hits/correct rejections) or red (misses/false alarms) for 100 msec. If participants did not respond within 1500 msec, a message prompted them to respond faster.

To keep the task engaging and equally difficult between both conditions, we used two online staircase procedures aimed at an average performance of 70%. This was done by adding Gaussian noise to the probe stimulus depending on individuals' psychometric functions estimated using Psychtoolbox QUEST algorithm (Farell & Pelli, 1999).

Eye Tracking Recording and Analysis

Gaze position was continuously tracked using an Eyelink 1000 (SR Research) eye tracker. A 13-point calibration was performed at the beginning of the experiment and after every third block. Gaze position was sampled at 1000 Hz.

Gaze data served to check for fixation throughout the memory and distractor presentation period (−1300 to −600 msec). Gaze position was baseline corrected by subtracting the median x and y coordinates during the baseline (−1800 to −1300 msec) from the entire trial. Trials were discarded from further analysis if fixation deviated more than 2° dva (x or y coordinates) from central fixation. An average of 7% of total trials across participants was removed at this stage. Four participants were excluded from further analysis because of a large number of eye movements (>25% trials removed) during stimulus encoding. A reanalysis of the data including these four participants resulted in qualitatively identical findings.

EEG Recording and Preprocessing

We recorded participants' EEG using a 64-channel Active-Two Biosemi system. Two additional electrodes placed on the outer eye canthus and above the left eye recorded horizontal and vertical eye movements. Data analysis was performed in MATLAB using the Fieldtrip toolbox. Before all preprocessing steps, we identified and removed bad channels via visual inspection. The EEG data were then re-referenced to the average of all channels, bandpass filtered between 0.5 and 80 Hz, and line noise was removed using a DFT filter (50 Hz). Thereafter, the data were epoched from 2.3 sec before flicker onset to 4 sec after flicker onset. Large movement-related artifacts were first removed through visual inspection. On average, 13% of trials were removed across participants at this stage. A subsequent independent component analysis on the separate data sets was used to remove components related to blinks and other high-frequency artifacts stemming from muscle activity. After EOG-based and EEG-based artifact removal, 80.91% of trials were considered for further processing. Finally, the data were downsampled to 512 Hz, and absolute baseline correction was performed (window −1800 to −1300 msec before flicker onset).

SSVEP and RESS

Frequency-specific SSVEP responses were isolated using a spatiotemporal source separation method (Cohen, 2022; Cohen & Gulbinaite, 2017), which is based on generalized eigenvalue decomposition and allows to maximize SNR of steady-state responses by exploiting information present in interchannel covariance matrices. Thus, instead of analyzing SSVEPs from a subset of electrodes with maximum power at the stimulation frequency, we analyzed a linearly weighted combination of signal from almost all electrodes. Notably, we removed a set ($n = 8$) of frontal channels (FP1, FPz, FP2, AF7, AF3, AFz, AF4, AF8) before the creation of spatial filters, as we expected a high amount of eye movement-related noise in these channels.

For each participant and stimulation frequency, a separate spatial filter was constructed by temporally narrow bandpass filtering (Gaussian filter) the raw data (X) around the stimulation frequency f (10 Hz or 13.333 Hz, FWHM = 0.666 Hz) and at the two neighboring frequencies ($f \pm 0.666$ Hz; FWHM = 0.666 Hz). All conditions were combined in the RESS analysis as the spatial location and therefore the EEG topography of the 10- and 13.333-Hz flicker were kept identical. Temporally filtered data (500–2000 msec relative to SSVEP onset) was then used to compute covariance matrices: one “signal” matrix (S covariance matrix) and two “reference” matrices that were averaged (R covariance matrix). The first 500 msec (0–500 msec) following SSVEP onset contain evoked potentials and thus were excluded to not compromise the quality of the spatial filter (Cohen & Gulbinaite, 2017). Generalized eigenvalue decomposition (MATLAB

function eig) performed on “signal” and “reference” covariance matrices returned matrices of eigenvalues and eigenvectors. To increase the robustness of the spatial filters, we applied a 1% shrinkage regularization to the average “reference” covariance matrix. Shrinkage regularization involves adding a percentage of the average eigenvalues onto the diagonals of the average “reference” covariance matrix (Cohen, 2022). This can reduce the influence of noise on the resulting eigen decomposition and has little other impact on the RESS results (Cohen, 2022). The eigenvectors (column vectors with values representing electrode weights, w) were used to obtain component time series (eigenvector multiplied by the original unfiltered single-trial time series, wTX).

The component with the highest SNR in the power spectra at the stimulation frequency was selected for further analysis. The topographical representation of each component was obtained by left-multiplying the eigenvector by the signal covariance matrix (wTS). The obtained topographical maps were normalized, and the sign of eigenvector was flipped for participants that showed spatial peaks opposite to that of the group average. The sign of the components affects only the representation of the topographical maps and has no effect on component time series (Cohen, 2022).

Differences in SSVEP responses associated with target and distractor locations were estimated by calculating power and coherence estimates at different stimulation frequencies. Power at each stimulation frequency was computed using the fast Fourier transform (FFT) on trial-averaged component time series in the 500–2000 msec time window (relative to the SSVEP onset) and zero-padded to obtain frequency resolution of 0.066 Hz. The absolute value of FFT coefficients was squared and averaged across trials. To facilitate comparison across SSVEPs elicited by different stimulation frequencies, SSVEP power values were expressed in SNR units:

$$\text{SNR}(f) = \frac{F(f)}{\frac{1}{2N} \sum_{k=\pm 6^*, \pm 7, \dots, \pm N} F(f + \Delta f \cdot k)}$$

where $N = \pm 2$ Hz, excluding 0.5 Hz around the frequency of interest. Individuals’ SNR values at 10 and 13.333 Hz were selected for further statistical assessment.

Time frequency decompositions were performed via continuous wavelet transformation. The phase-locked power during SSVEP stimulation was calculated by multiplying the power spectrum of trial-averaged component time series with the power spectrum of complex Morlet wavelets ($e^{i2\pi ft} e^{-t^2/(2\sigma^2)}$), where t is time, f_i is frequency that ranged from 2 to 20 Hz in 0.333-Hz steps, and σ is the width of each frequency band defined as $\sigma = f_i/n$, where n is a number of wavelet cycles that we set to $n = 7$. The resulting frequency smearing was 1.42 Hz (at 10 Hz) and 1.9 Hz (at 13 Hz).

Coherence was estimated between the single-trial component time series and pure sine waves (10 and

13.333 Hz). First, we filtered 6300-msec epochs using a phase preserving, two-pass, Butterworth bandpass filter (fourth order) with a Hamming taper. The center filter frequencies were set to 10 and 13.333 Hz, respectively, with a passband of ± 1 Hz. We then determined the analytic signal by the Hilbert transform, which was subsequently used as the input for coherence at time point t (adopted from Pan, Frisson, & Jensen, 2021):

$$\text{coh}(t) = \frac{\left| n^{-1} \sum_{j=1}^n m_{x_j}(t) m_{y_j}(t) e^{i\phi_{xy}(t)} \right|^2}{n^{-1} \sum_{j=1}^n m_{x_j}(t)^2 m_{y_j}(t)^2}$$

where j is the trial, n is the number of trials, $m_x(t)$ and $m_y(t)$ are the time-varying magnitude of the analytic signals from single-trial component time series and pure sine waves, and $\phi_{xy}(t)$ is the phase difference as a function of time between them.

Statistical Analysis

To estimate the effect of internal attention on oscillatory power (SNR) in the one-item and two-item conditions, we calculated attentional modulation indices (AMIs; Zhigalov & Jensen, 2020) for both frequencies (10 and 13.333 Hz, estimated with separate spatial filters) using the following formula:

$$\text{AMI} = \frac{\left(\text{SNR}(f)_{\text{memory}} - \text{SNR}(f)_{\text{distractor}} \right)}{\left(\text{SNR}(f)_{\text{memory}} + \text{SNR}(f)_{\text{distractor}} \right)}$$

The AMI in the one-item condition was calculated using the SNR measured from the memory and the distractor locations in the one-item condition. The AMI in the two-item condition was calculated using the SNR measured from one of two memory locations in the two-item condition and the distractor location in the one-item condition. The resulting indices were then statistically tested using a two-way ANOVA with factors Load (1 and 2) and Frequency (10 and 13.333 Hz) and t tests.

Coherence time series in one- and two-item conditions were statistically assessed using a nonparametric cluster-based permutation test (Maris & Oostenveld, 2007). To this end, we first calculated individual participants coherence time series in the one-item condition at 10 and 13.333 Hz, which reflects processing at memory and distractor locations. This resulted in four coherence time series (10-Hz memory, 10-Hz distractor, 13.333-Hz memory, 13.333-Hz distractor). This analysis was repeated for the two-item condition, resulting in two coherence time series (10-Hz memory, 13.333-Hz memory). To test if coherence time series significantly differed between memory locations (one-item and two-item conditions, respectively) compared with distractor locations (one-item condition), we first calculated the veridical difference in cluster-level t mass between two conditions. This was done by running t tests for every individual time point of

the group-level difference time series and identifying clusters of consecutive time points where the p value fell below $\alpha = .05$. The t values within the largest cluster were summed to calculate the cluster-level t mass. We then randomly swapped 50% of labels in both conditions and recalculated the difference in largest cluster-level t mass. This procedure was repeated 10,000 times and generated the distribution that would be expected under the null hypothesis (H0: Distribution of distance-to-bound score t -mass differences do not differ significantly between conditions). The veridically observed t -mass difference was compared with the null distribution of t -mass differences, and the null hypothesis was rejected if it exceeded the 95% quantile.

RESULTS

Load Impacts Behavioral Performance

As expected, behavioral performance was lower with two to-be-memorized items than with one to-be-memorized item, expressing itself in a significantly lower hit rate, $t(22) = 7.05, p < .01$ (Figure 2A); longer RTs, $t(22) = 5.52, p < .01$ (Figure 2B); and higher false alarm rate (FAR), $t(22) = 9.06, p < .01$ (Figure 2B) in the condition in which two items needed to be memorized.

Importantly, the seemingly high FARs of 44.8%/28.1% observed in our experiment can be explained by our specific task design. Orientations of memory stimuli were drawn from a set of six equally spaced orientations, and the orientation of the probe in catch trials was drawn from one of the remaining four orientations. This means that the orientation of the probe is adjacent to one of the memory stimuli in 69% of trials, leading to an a priori FAR of 69% if participants' memory fidelity is too poor to distinguish adjacent orientations. Notably, if the same participant were able to distinguish orientations separated by two steps, they would still be able to differentiate between 75% of orientation combinations and perform the task. The high FAR observed in our task is therefore a result

of the relatively high confusability of adjacent orientations. This is also supported by the fact that FAR is monotonously decreasing as a function of the difference between memory and distractor orientation (30 vs. 90, $p = .0004$; 30 vs. 60, $p = .0017$; 60 vs. 90, $p = .0037$; Figure 2C).

Dynamic Allocation of Spatial Attention during VWM Maintenance

We hypothesized that SSVEP responses corresponding to memory locations would be enhanced compared with distractor locations, reflecting the allocation of internal attention to the currently maintained VWM representation. Spectral analysis of 10- and 13-Hz component time series (500–2000 msec) revealed oscillatory peaks at the corresponding frequencies (Figure 4A, B). Topographic representations of subject average spatial filter maps for each SSVEP component (10 and 13 Hz) show expected lateralization in scalp projections (Figure 4A, B).

To investigate the time course of allocation of attention, we compared SSVEP coherence time series and time-resolved spectral power at frequencies corresponding to memory (Load 1 and Load 2) and distractor locations. Notably, spectral power of trial-averaged time series is typically analyzed in SSVEP studies, but phase-based intertrial measures such as coherence have been applied as well and can provide a more robust estimate of the tagged signal that is less influenced by high-power artifacts and variability between participants (Minarik, Berger, & Jensen, 2023; Yang, Paller, & van Vugt, 2022; Schneider et al., 2017; Knight, Marsh, Brewer, & Clementz, 2012). Here, we perform both types of analysis for completeness. Cluster-based permutation tests revealed significantly higher 13-Hz coherence at memory locations in the one-item and two-item conditions when individually compared with the distractor location in the one-item condition (Load 1, 1200–1950 msec; Load 2, 1350–2000 msec; Figure 3B). We found no significant differences in 13-Hz coherence at memory locations between conditions Load 1 and Load

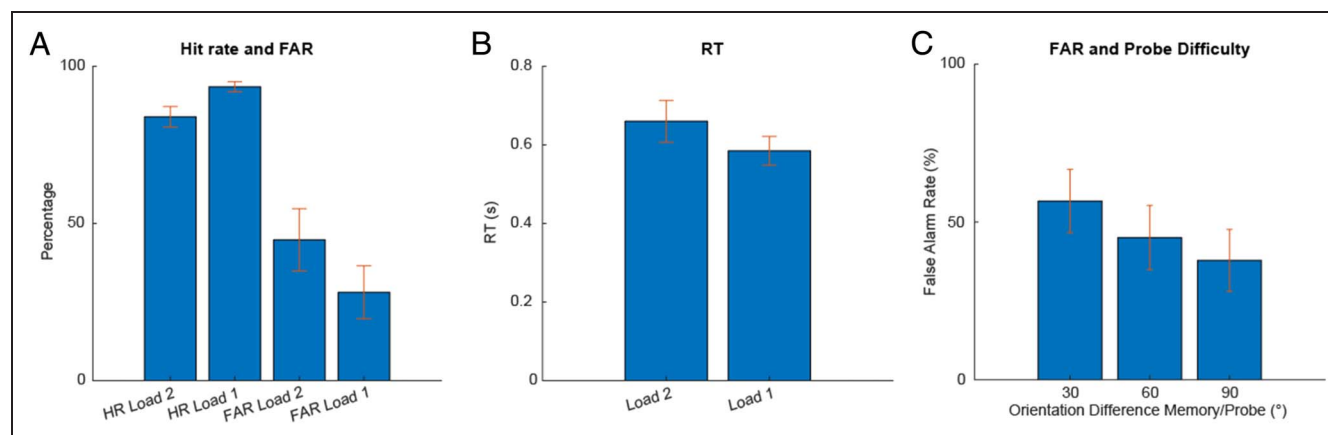


Figure 2. Behavioral results. (A, B) Group average performance (hit rates and FARs) as well as RTs for Load 1 and Load 2 conditions. (C) FAR depending on orientation difference between memory and probe. Whiskers indicate upper and lower 95% confidence intervals.

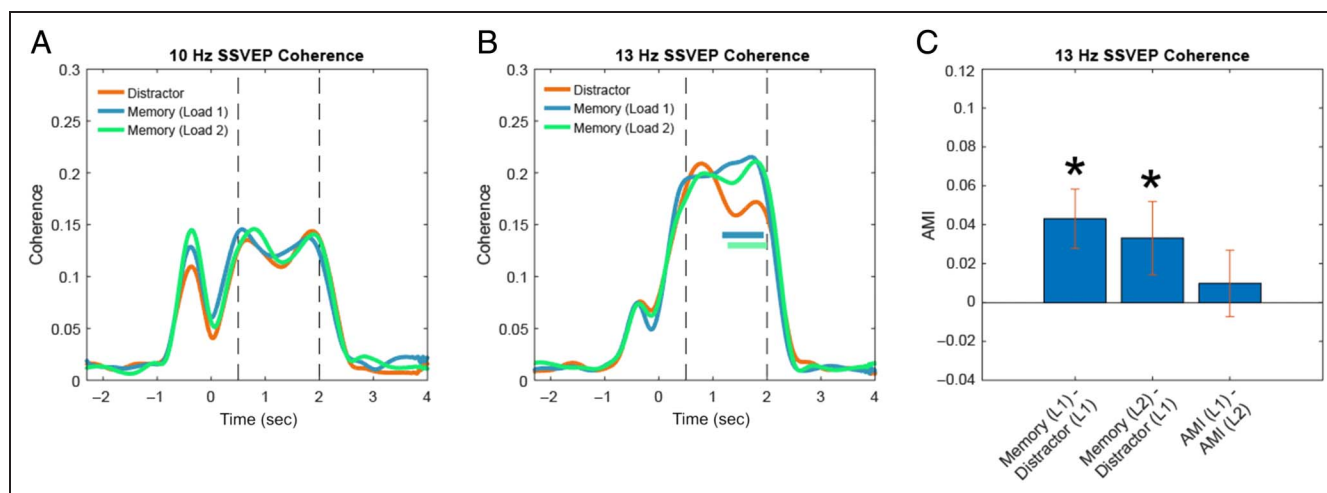


Figure 3. (A) 10-Hz coherence over time. Orange line indicates coherence over trials in which the item at the 10-Hz tagged location was a distractor. Similarly, blue and green lines indicate coherence corresponding to 10-Hz tagged memory locations in Load 1 (blue) and Load 2 (green) conditions. Blue and green bars show clusters indicating significant differences between memory (Load 1) and distractor locations (blue), and memory (Load 2) and distractor locations (green). Black dotted lines indicate SSVEP time window of interest (B) Same as A but for 13-Hz coherence. (C) 13-Hz coherence AMI averaged within significant cluster (1350–1950 msec). Error bars indicate 95% confidence interval. Coherence significantly drops for distractor against memory locations before probe presentation.

2. Furthermore, permutation tests revealed no significant differences between memory and distractor locations for 10-Hz coherence time series (Figure 3A). To adjust for potential differences in individual's absolute coherence, we calculated normalized AMI (see Statistical Analysis under Methods section). Coherence values were averaged within significant time windows identified by the cluster-based permutation test (1350–1950 msec), and AMIs (Figure 3C) were calculated as follows:

$$\text{Memory (L1) - Distractor (L1)} \\ : \frac{\text{Memory (Load 1) - Distractor (Load 1)}}{\text{Memory (Load 1) + Distractor (Load 1)}}$$

$$\text{Memory (L2) - Distractor (L1)} \\ : \frac{\text{Memory (Load 2) - Distractor (Load 1)}}{\text{Memory (Load 2) + Distractor (Load 1)}}$$

In addition, we quantified the difference between the so calculated AMIs:

$$\text{AMI (L1) - AMI (L2)} \\ : \frac{\text{Memory (L1) - Distractor (L1)} - \text{Memory (L2) - Distractor (L1)}}{\text{Memory (L1) - Distractor (L1)} + \text{Memory (L2) - Distractor (L1)}}$$

As expected, AMIs calculated from 13-Hz coherence was significantly larger than zero for Load 1/Distractor, $t(22) = 3.97$, $p < .001$, and Load 2/Distractor, $t(22) = 3.01$, $p = .007$, indicating a stronger allocation of attention to previous memory as compared with distractor locations. We found no significant differences in the AMI calculated from 13-Hz coherence between Load 1 and Load 2 memory conditions, $t(22) = 1.98$, $p = .06$ (Figure 3C), indicating that the degree of attentional allocation to a single location was not dependent on the total number of items in VWM.

Furthermore, AMIs calculated from 10-Hz coherence did not differ significantly from zero in Load 1/Distractor ($p = .72$), Load 2/Distractor ($p = .96$), or when comparing between both ($p = .75$; Figure 3C).

We verified that the observed differences in SSVEP responses were not caused by participants moving their eyes closer to the memory location during the SSVEP interval. This was done by comparing horizontal eye position when memory items were encoded left or right of fixation in the one-item condition, as well as when two items were encoded laterally in the two-item condition. Cluster-based permutation tests performed on the time series differences calculated between all three conditions (Item Right – Item Left, Item Right – Item Left + Right, Item Right + Left – Item Left; Figure 5C) revealed no significant clusters, suggesting that horizontal eye position did not differ between conditions.

In addition to coherence, we analyzed the temporal dynamics of the SSVEP components by quantifying spectral power over time. SSVEPs are conventionally investigated using the power calculated from trial-averaged time series (Vissers, Gulbinaite, van den Bos, & Slagter, 2017; Peterson et al., 2014; Wu, Yao, Tang, Huang, & Su, 2010; Ellis, Silberstein, & Nathan, 2006; Perlstein et al., 2003; Silberstein, Nunez, Pipingas, Harris, & Danieli, 2001). This additional analysis was therefore performed to facilitate comparability with the literature. 10-Hz and 13-Hz power envelopes (Figure 4D, E) were extracted from corresponding time–frequency representations of trial-averaged component time series (Figure 4G, H), and averaging power values centered around 10 and 13.333 Hz (± 1 Hz) over time. Cluster-based permutation tests were performed to compare time-resolved power of memory (Load 1 and Load 2) and distractor locations.

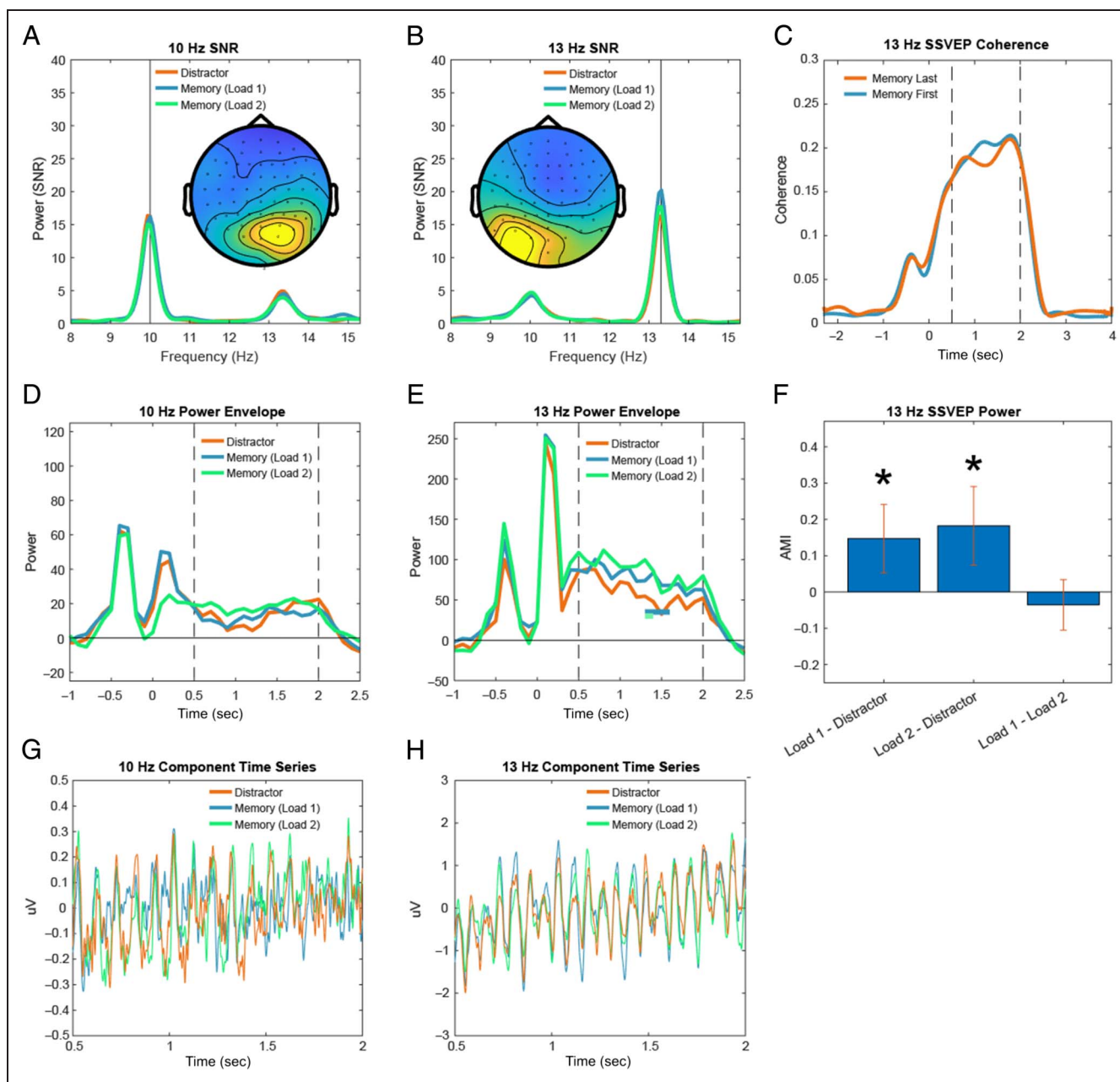


Figure 4. (A, B) Signal-to-noise spectra of SSVEP component time series. Topographies display subject-averaged filter maps for 10- and 13-Hz components, respectively. (C) 13-Hz coherence over time. Orange line indicates coherence over trials in which the item at the 13-Hz tagged location was presented last. Blue line indicates coherence over trials in which the item at the 13-Hz tagged location was presented first. (D) 10-Hz power over time. Orange line indicates power in trials in which the item at the 10-Hz tagged location was a distractor. Similarly, blue and green lines indicate power corresponding to 10-Hz tagged memory locations in Load 1 (blue) and Load 2 (green) conditions. Blue and green bars show clusters indicating significant differences between memory (Load 1) and distractor locations (blue), and memory (Load 2) and distractor locations (green). Black dotted lines indicate SSVEP time window of interest. (E) Same as D but for 13-Hz power. (F) 13-Hz power AMI averaged within significant cluster (1350–1950 msec). Whiskers indicate 95% confidence interval. (G, H) 10- and 13-Hz RESS component time series.

Permutation tests revealed significantly higher 13-Hz power at memory locations (Load 1, 1300–1500 msec; Load 2, 1300–1400 msec) compared with distractor locations (Figure 4E), but no differences in 10-Hz power between conditions (Figure 4D). Notably, the temporal profiles of 13-Hz coherence and power differed such that coherence generally increased over time whereas power decreased over time. AMIs calculated from

13-Hz power were significantly larger than zero for Load 1/Distractor, $t(22) = 3.24, p = .004$, and Load 2/Distractor, $t(22) = 3.50, p = .002$, but did not differ between the two, $t(22) = -1.06, p = .30$ (Figure 4F). Furthermore, AMIs of 10-Hz components did not differ significantly from zero in Load 1 minus Distractor, $t(22) = -1.38, p = .18$; Load 2 minus Distractor, $t(22) = 1.4, p = .17$; or when comparing between both,

$t(22) = -1.75, p = .93$ (Figure 4F). Taken together, our findings show that 13-Hz SSVEP responses dynamically indexed the allocation of spatial attention to both memory and distractor locations. When spatial locations were previously occupied by a memory and a distractor item, respectively, spatial attention remained on the memory location whereas it dropped off at the distractor location shortly before probe comparison. When two spatial locations were occupied by memory items, attention remained on both locations. Last, we found no differences in the amount of attention allocated to individual locations when one versus two items were maintained in memory.

Location-specific Effects on SSVEPs Are Not Explained by Attention during Encoding

The effects of memory location on SSVEP responses could be explained either by sustained attention directed toward the item location in working memory or alternatively by persisting aftereffects of spatial attention during stimulus encoding. We reasoned that potential aftereffects of spatial attention during encoding should be stronger (or

longer lasting) for locations where the last item was encoded as compared with locations where the first item was encoded. To test this prediction, we divided 13-Hz component time series in the two-item condition into two sets of trials. In the first set of trials, memory items were encoded first at the 13-Hz stimulation location (memory first) whereas in the second set, memory items were encoded last at the 13-Hz location (memory last). Lingering aftereffects of attention during encoding should hence manifest as stronger coherence in memory last trials. Cluster-based permutation tests revealed no significant differences between memory first and memory last, suggesting that location-specific effects on SSVEP coherence were not caused by potential aftereffects of spatial attention during encoding.

Reallocation of Spatial Attention Predicts RTs

The observed pattern of SSVEP responses indicates that spatial attention was maintained on both memory and distractor locations but reduced sharply at distractor locations shortly before the presentation of the probe in the center of the screen. We hypothesized that this reduction

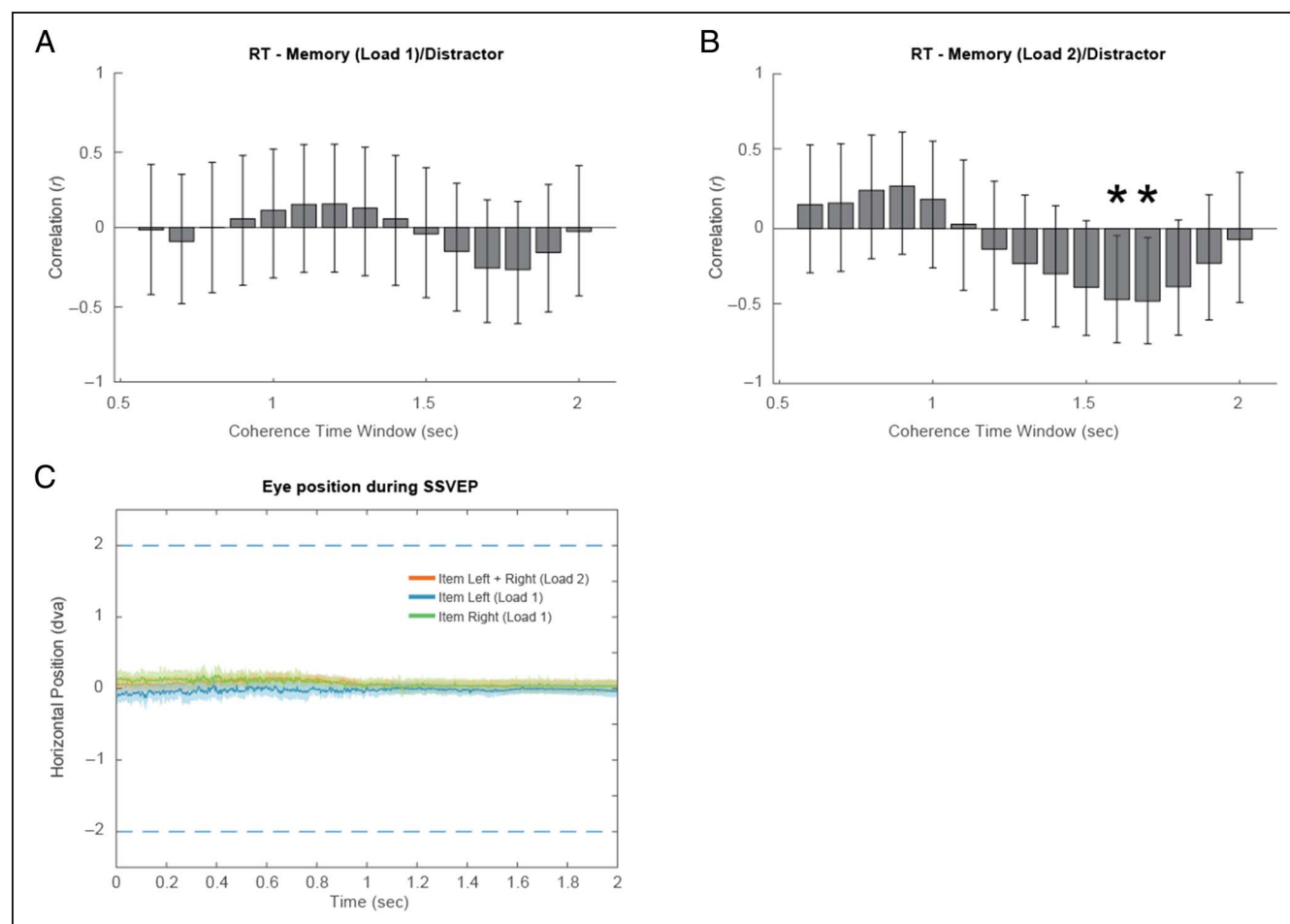


Figure 5. (A, B) Pearson correlations between AMLs over time (100-msec bins) and average RTs. Significant time bins in B: 1700 msec ($p = .032$) and 1800 msec ($p = .028$). Whiskers indicate upper and lower 95% confidence intervals. (C) Horizontal eye position during SSVEP window. Shaded areas indicate upper and lower 95% confidence intervals.

might be the result of a reallocation of attention from the distractor location to the center of the screen to facilitate perception of the probe. Simultaneously, attention might remain on the memory location as this could be a prerequisite for VWM maintenance.

To investigate whether the reallocation of attention from distractor to probe had a meaningful behavioral effect, we correlated individual participants' coherence AMIs (Load 1/Distractor, Load 2/Distractor) at each time point with individuals' average RTs. We hypothesized that a stronger reallocation of attention should lead to a more efficient perceptual processing of the probe stimulus and reduce RTs. Coherence AMIs in the Load 2/Distractor condition at multiple successive time points shortly before probe appearance (1700–1800 msec) were significantly negatively correlated with RTs (Figure 5B). We observed a highly similar pattern of correlations in the Load 1/Distractor condition, although it did not reach statistical significance. We repeated this analysis using only RTs of trials with correct responses, leading to an almost identical pattern of correlations, reaching significance at 1700 ($p = .031$) and 1800 msec ($p = .028$). These results suggest that attention was reallocated from the distractor location to the central probe location and that stronger shifts led to faster responses to the probe.

DISCUSSION

We here used SSVEPs to measure the dynamic allocation of attention to to-be-memorized gratings and to-be-ignored distractors memory items by exploiting that items were encoded (and maintained) spatially, even though space was behaviorally irrelevant to answer the probe. We tested whether memory locations were attended more strongly than distractor locations, how attention was distributed between more than one memory location, and how attention was reallocated on a highly resolved timescale in anticipation of a central probe. Our findings show that SSVEP responses dynamically indexed the allocation of spatial attention to both memory and distractor locations. When both locations were occupied by memory items, attention was sustained on both. However, when one location was previously occupied by a distractor item, spatial attention remained on the memory location but dropped off at the distractor location shortly before probe comparison. The degree of this reduction predicted RTs—indicating that the reallocation of attention from irrelevant distractor to relevant upcoming probe location determines accurate retrieval and responding.

The central strength of our paradigm lies in its ability to demonstrate how attention is dynamically allocated to several relevant and irrelevant spatial locations during a VWM task. Recent work has highlighted the importance of studying working memory as a dynamic process that flexibly adjust to the current task goals (Nobre & van Ede, 2023; Buschman & Miller, 2022; Chota & Van der Stigchel, 2021). Previous behavioral work has relied primarily on

probe stimuli to measure item location-specific attentional effects (Chen & Wyble, 2015; Elsley & Parmentier, 2015; Theeuwes et al., 2011; Awh & Jonides, 2001; Awh et al., 1998). Although informative about the effects on perception, this approach is inherently limited in its ability to uncover dynamical changes in attention as only single time points can be probed per trial. Experiments using classic electrophysiological correlates such as alpha lateralization (Liu et al., 2022, 2023; Foster et al., 2017; Poch et al., 2014, 2017; van Ede et al., 2017) or time-resolved behavioral measures such as eye movements (van Ede et al., 2019, 2020, 2021) attempt to paint a more dynamic picture of attention but ultimately only provide correlational evidence for its effects on perceptual processing. In contrast, the SSVEP paradigm utilized here provides a highly time-resolved and functionally direct estimate of how attention modulates spatially specific perceptual processing. Moreover, we could measure attentional allocation without using behavioral probes at memory or distractor locations. This uniquely allowed us to test attentional facilitation without participants explicitly directing spatial attention to potential probe locations and hence isolate memory-specific attention.

One of the more surprising results in this experiment is the fact that distractor locations were attended for almost 2100 msec after the distractor was presented. We propose several possible explanations for this, which might not be mutually exclusive. First, participants might have accidentally encoded distractors in VWM because of attention automatically being captured by the abrupt onset, the relatively short presentation time (300–600 msec), and no prior knowledge on the upcoming location of the relevant memory item. Previous work showed such occasional encoding and maintenance of distractors for more than a second, even with predictable spatial location (Vogel, McCollough, & Machizawa, 2005). The sustained increase in perceptual processing at distractor locations might therefore index a similar engagement of spatial attention as found during memory maintenance. While maintaining distractors attended in VWM might seem counterintuitive, the active removal of items from VWM and hence from the focus of spatial attention could be more effortful than simply maintaining them in memory. Only when attentional resources are required elsewhere, in our case when probe presentation is imminent, attention would then be reallocated from the encoded distractor to more relevant locations. An additional explanation for the sustained attention directed to distractor locations is that the flickering stimuli themselves exogenously attracted attention, which led to a saturation of the SSVEP response measured on the scalp. This could also explain why we do not see a general reduction in SSVEP coherence in the two-item condition in which attentional resources also would have to be dedicated to the probe location shortly before its appearance. Under this assumption, the reduction in SSVEP coherence at the distractor location might reflect the active suppression or removal of the accidentally encoded distractor

item from memory, leading to a strong reduction in attention directed to its former location. Similar to our initial hypothesis, this would also provide a parsimonious explanation for the link between SSVEP responses and RTs, as the inhibited item might free up working memory capacity for the upcoming probe. Notably, the link between relative memory/distractor coherence (AMI) and RTs was stronger when the AMI was derived from the two-item condition as compared with the one-item condition, potentially attributable to a lack of sensitivity of our measurement tool and/or a small sample size. In their essence, these two explanations point to two distinct models of attention in working memory: In the first model, attentional resources are deliberately allocated and reallocated between encoded items. In the second model, available attentional resources are automatically distributed between all encoded items and reallocation entails the active inhibition and/or removal of items from the pool of memories. Future work will have to dissociate between these two models by adding flicker locations at which neither memory nor distractor items are presented.

SSVEPs have been used as a technique to study VWM in a number of ways (Thigpen, Petro, Oswald, Oberauer, & Keil, 2019; Vissers et al., 2017; Peterson et al., 2014; Wu et al., 2010; Ellis et al., 2006; Perlstein et al., 2003; Silberstein et al., 2001). Many of these studies used diffuse full-field flicker to investigate brain dynamics during VWM operations (Wu et al., 2010; Ellis et al., 2006; Perlstein et al., 2003; Silberstein et al., 2001). Although full-field flicker does not allow for memory/distractor item-specific tagging, it provided first evidence that SSVEP responses are increased in VWM maintenance. Increased SSVEP responses, in turn, are likely to be interpreted as a sign of increased attention toward the external world. Here, we attempted to exploit this putative mechanism by measuring attentional allocation to spatially specific internal representations, that is, memory items that were presented at the exact locations of flickering discs.

To our knowledge, there is only a single study that has used SSVEPs to individually probe attention directed to former memory and distractor locations during the maintenance interval (Vissers et al., 2017). The authors found no attentional effect of memory versus distractor locations at the entrained frequencies of 16/18 Hz but revealed larger amplitudes for memory locations at the second harmonic (32/36 Hz), in line with our results. They hypothesized that the attentional effect might not have been revealed at the entrainment frequencies because the placeholders instead of precise stimulus locations were flickered. This might have led to a surround suppression and subsequently a reduction in amplitude of the flicker signal. Notably, the probes in their study were presented at locations that overlapped with the memory/distractor items—spatial attention to the memorized items and to the upcoming probes can therefore hardly be dissociated. Although Vissers et al. (2017) did not statistically assess dynamic changes in attention during the maintenance

period, visual inspection of the SSVEP signal over time indicates a reduction in attention over distractor locations ~ 1000 msec before probe onset, which tightly resembles the attentional reallocation demonstrated in our work. Together with the presently reported data, this provides converging evidence that spatial attention dynamically modulates SSVEP responses during VWM maintenance.

How are attentional resources distributed between one or more relevant memory locations during maintenance? Previous work has shown that SSVEP amplitude is reduced when attention is distributed between two instead of one relevant location (Andersen et al., 2009; Toffanin et al., 2009). In contrast, we found no differences in SSVEP responses between one-item and two-item conditions. This discrepancy might be due to both studies using external distractors that had to actively be ignored. When presented with two competing streams of external information, the visual system might benefit from dedicating additional resources to the attended location. Spatial attention might therefore be redistributed only to the attended visual stream leading to increased SSVEP responses. In our study, there was no competing stream of external visual information that had to be actively suppressed, which might have made it less important to redirect additional attentional resources to the relevant memory location. This interpretation is in line with the hypothesis that attention plays an important role in protecting memorized and perceived neural representations from external interference (Souza & Oberauer, 2016). Future studies might introduce more interfering distractors in the maintenance period to test if attentional allocation changes as a function of external distractor load.

One could argue that the location-specific effects observed here are not specific to memory maintenance or retrieval but rather reflect lingering attentional effects caused by stimulus encoding. We believe this to be unlikely: First, one would expect encoding-related effects to be most prominent at the location of the last item and weakest at the location of the first item. We explicitly tested this by comparing coherence between trials in which the first or the second item was presented at the 13-Hz SSVEP location, finding no effect of encoding order. Second, attentional facilitation caused by attentional orienting to peripheral cues has been shown to peak around 175 msec and does generally not last longer than 400 msec (Müller & Rabbitt, 1989), whereas we found the strongest facilitation to emerge at around 1800 msec.

Although we observed a consistent effect of memory/distractor location on 13-Hz SSVEP responses, we did not find similar effects for 10-Hz responses. This might be explained by the fact that 10-Hz entrainment interferes with the brain's endogenous alpha rhythms, which can be found at similar frequencies (Gulbinaite et al., 2017, 2019; Keitel et al., 2019). Previous work has shown that either an increase or decrease in flicker amplitude in the alpha range can be observed, depending on the individual peak

alpha frequency of the participant and the strength of endogenous alpha oscillations (Gulbinaite et al., 2019; Wang, Clementz, & Keil, 2007; Ding, Sperling, & Srinivasan, 2006). Endogenous alpha oscillations have been demonstrated to decrease over visual areas contralateral to the attended hemifield and hemifields where memory items were encoded (Liu et al., 2023; Poch et al., 2014, 2017; Ikkai, Dandekar, & Curtis, 2016; Gould, Rushworth, & Nobre, 2011; Grent-'t-Jong, Boehler, Kenemans, & Woldorff, 2011; Kelly, Gomez-Ramirez, & Foxe, 2009; Siegel, Donner, Oostenveld, Fries, & Engel, 2008; Thut, Nietzel, Brandt, & Pascual-Leone, 2006; Sauseng et al., 2005). The lack of an effect at 10 Hz might therefore be the result of contralateral increases in the rhythmic responses to the flicker stimulus and simultaneous contralateral decreases in endogenous alpha oscillations. The effect of attention on alpha oscillations measured during rhythmic brain stimulation critically depends on the type of analysis that is performed. Spectral analysis of the phase-locked trial-averaged EEG signal as well as phase-based measures such as coherence, both of which were performed here, usually show an increase in oscillatory amplitude and/or phase consistency as a result of attention (Keitel et al., 2019). In contrast, analysis of total power via averaging of single-trial spectrograms tends to show a reduction in signal amplitude caused by attention. Although both of our analyses (phase-locked power and coherence) of the SSVEP component time series should show an increase because of attention, the spatial RESS filters were calculated from the entire concatenated EEG signal and might therefore also be sensitive to non-phase-locked (endogenous) oscillatory activity. Therefore, the selection of RESS components was based on the phase-locked power of individual components time series and the spatial filter weights were strongest over contralateral channels (Figure 4A, B), suggesting that the influence of non-phase-locked oscillatory activity was minimal. Future work should choose frequencies outside the range of endogenous oscillations to disentangle the opposing effects of attention on endogenous and stimulus-evoked rhythmic activity.

Our results provide further evidence to the idea that visual memoranda are stored in a spatially organized format (van Ede et al., 2019; Schneegans & Bays, 2017). Furthermore, our findings are in line with the sensory recruitment hypothesis claiming that visual sensory areas, which are largely retinotopically organized, are involved in the maintenance of memoranda (Rademaker, Chunharas, & Serences, 2019; Ester, Rademaker, & Sprague, 2016; Ester, Serences, & Awh, 2009; Harrison & Tong, 2009; Serences, Ester, Vogel, & Awh, 2009). The spatial organization of the visuo-attentional system is assumed to play a key role in the perceptual binding of multiple features into objects (Kahneman, Treisman, & Gibbs, 1992; Treisman, 1988). Our findings support the idea that this also extends to objects stored in memory because spatial attentional effects could be observed despite “external” memory

locations remaining completely irrelevant throughout our experiment.

In conclusion, we show that SSVEPs are a powerful new tool to study dynamic changes in internal attention directed toward individual representations in VWM. This was only possible as spatial locations of encoded items were irrelevant to answer probes—supporting the notion of a spatially organized VWM. We demonstrate that VWM maintenance and utilization is accompanied by dynamic, location-specific, and behaviorally relevant (re)distribution of attention indexed by SSVEP coherence. Crucially, although spatial attention is continuously maintained on memory locations, it is reallocated from distractor to a central location to facilitate encoding of the probe leading to faster RTs.

Corresponding author: Samson Chota, Utrecht University, Heidelberglaan 8, 3584 CS Utrecht, the Netherlands, or via e-mail: s.chota@uu.nl.

Data Availability Statement

The data and analysis pipeline are available via OSF under the following link: <https://osf.io/39g4w/>.

Author Contributions

Samson Chota: Conceptualization; Formal analysis; Investigation; Methodology; Supervision; Writing—Original draft; Writing—Review & editing. Arnaud T. Bruat: Formal analysis; Investigation. Stefan Van der Stigchel: Conceptualization; Funding acquisition; Supervision; Writing—Review & editing. Christoph Strauch: Conceptualization; Writing—Original draft; Writing—Review & editing.

Funding Information

This project has received funding from the European Research Council under the European Union’s Horizon 2020 Research and Innovation Programme (grant agreement no. 863732).

Diversity in Citation Practices

Retrospective analysis of the citations in every article published in this journal from 2010 to 2021 reveals a persistent pattern of gender imbalance: Although the proportions of authorship teams (categorized by estimated gender identification of first author/last author) publishing in the *Journal of Cognitive Neuroscience (JoCN)* during this period were $M(an)/M = .407$, $W(oman)/M = .32$, $M/W = .115$, and $W/W = .159$, the comparable proportions for the articles that these authorship teams cited were $M/M = .549$, $W/M = .257$, $M/W = .109$, and $W/W = .085$ (Postle and Fulvio, *JoCN*, 34:1, pp. 1–3). Consequently, *JoCN* encourages all authors to consider gender balance explicitly when

selecting which articles to cite and gives them the opportunity to report their article's gender citation balance.

REFERENCES

- Andersen, S. K., Müller, M. M., & Hillyard, S. A. (2009). Color-selective attention need not be mediated by spatial attention. *Journal of Vision*, *9*, 2. <https://doi.org/10.1167/9.6.2>, PubMed: 19761293
- Awh, E., & Jonides, J. (2001). Overlapping mechanisms of attention and spatial working memory. *Trends in Cognitive Sciences*, *5*, 119–126. [https://doi.org/10.1016/S1364-6613\(00\)01593-X](https://doi.org/10.1016/S1364-6613(00)01593-X), PubMed: 11239812
- Awh, E., Jonides, J., & Reuter-Lorenz, P. A. (1998). Rehearsal in spatial working memory. *Journal of Experimental Psychology: Human Perception and Performance*, *24*, 780–790. <https://doi.org/10.1037/0096-1523.24.3.780>, PubMed: 9627416
- Awh, E., Vogel, E. K., & Oh, S.-H. (2006). Interactions between attention and working memory. *Neuroscience*, *139*, 201–208. <https://doi.org/10.1016/j.neuroscience.2005.08.023>, PubMed: 16324792
- Baddeley, A. (1992). Working memory. *Science*, *255*, 556–559. <https://doi.org/10.1126/science.1736359>, PubMed: 1736359
- Brainard, D. H. (1997). The psychophysics toolbox. *Spatial Vision*, *10*, 433–436. <https://doi.org/10.1163/156856897X00357>, PubMed: 9176952
- Buschman, T. J., & Miller, E. K. (2022). Working memory is complex and dynamic, like your thoughts. *Journal of Cognitive Neuroscience*, *35*, 17–23. https://doi.org/10.1162/jocn_a_01940, PubMed: 36322832
- Chen, H., & Wyble, B. (2015). The location but not the attributes of visual cues are automatically encoded into working memory. *Vision Research*, *107*, 76–85. <https://doi.org/10.1016/j.visres.2014.11.010>, PubMed: 25490435
- Chota, S., & Van der Stigchel, S. (2021). Dynamic and flexible transformation and reallocation of visual working memory representations. *Visual Cognition*, *29*, 409–415. <https://doi.org/10.1080/13506285.2021.1891168>
- Chota, S., & Van der Stigchel, S. (2022). Attention samples features in working memory rhythmically. *Journal of Vision*, *22*, 3485. <https://doi.org/10.1167/jov.22.14.3485>
- Christophel, T. B., Hebart, M. N., & Haynes, J.-D. (2012). Decoding the contents of visual short-term memory from human visual and parietal cortex. *Journal of Neuroscience*, *32*, 12983–12989. <https://doi.org/10.1523/JNEUROSCI.0184-12.2012>, PubMed: 22993415
- Cohen, M. X. (2022). A tutorial on generalized eigendecomposition for denoising, contrast enhancement, and dimension reduction in multichannel electrophysiology. *Neuroimage*, *247*, 118809. <https://doi.org/10.1016/j.neuroimage.2021.118809>, PubMed: 34906717
- Cohen, M. X., & Gulbinaite, R. (2017). Rhythmic entrainment source separation: Optimizing analyses of neural responses to rhythmic sensory stimulation. *Neuroimage*, *147*, 43–56. <https://doi.org/10.1016/j.neuroimage.2016.11.036>, PubMed: 27916666
- Dell'Acqua, R., Sessa, P., Toffanin, P., Luria, R., & Jolicoeur, P. (2010). Orienting attention to objects in visual short-term memory. *Neuropsychologia*, *48*, 419–428. <https://doi.org/10.1016/j.neuropsychologia.2009.09.033>, PubMed: 19804791
- Ding, J., Sperling, G., & Srinivasan, R. (2006). Attentional modulation of SSVEP power depends on the network tagged by the flicker frequency. *Cerebral Cortex*, *16*, 1016–1029. <https://doi.org/10.1093/cercor/bhj044>, PubMed: 16221931
- Eimer, M., & Kiss, M. (2010). An electrophysiological measure of access to representations in visual working memory. *Psychophysiology*, *47*, 197–200. <https://doi.org/10.1111/j.1469-8986.2009.00879.x>, PubMed: 19674389
- Ellis, K. A., Silberstein, R. B., & Nathan, P. J. (2006). Exploring the temporal dynamics of the spatial working memory *n*-back task using steady state visual evoked potentials (SSVEP). *Neuroimage*, *31*, 1741–1751. <https://doi.org/10.1016/j.neuroimage.2006.02.014>, PubMed: 16580845
- Elsley, J. V., & Parmentier, F. B. R. (2015). The asymmetry and temporal dynamics of incidental letter–location bindings in working memory. *Quarterly Journal of Experimental Psychology*, *68*, 433–441. <https://doi.org/10.1080/17470218.2014.982137>, PubMed: 25482047
- Engbert, R., & Kliegl, R. (2003). Microsaccades uncover the orientation of covert attention. *Vision Research*, *43*, 1035–1045. [https://doi.org/10.1016/S0042-6989\(03\)00084-1](https://doi.org/10.1016/S0042-6989(03)00084-1), PubMed: 12676246
- Ester, E. F., Rademaker, R. L., & Sprague, T. C. (2016). How do visual and parietal cortex contribute to visual short-term memory? *eNeuro*, *3*, ENEURO.0041-16.2016. <https://doi.org/10.1523/ENEURO.0041-16.2016>, PubMed: 27294194
- Ester, E. F., Serences, J. T., & Awh, E. (2009). Spatially global representations in human primary visual cortex during working memory maintenance. *Journal of Neuroscience*, *29*, 15258–15265. <https://doi.org/10.1523/JNEUROSCI.4388-09.2009>, PubMed: 19955378
- Farell, B., & Pelli, D. (1999). Psychophysical methods, or how to measure a threshold, and why. In R. Carpenter & J. Robson (Eds.), *Vision Research: A Practical Guide to Laboratory Methods* (pp. 129–136). Oxford Academic. <https://doi.org/10.1093/acprof:oso/9780198523192.003.0005>
- Foster, J. J., Bsaies, E. M., Jaffe, R. J., & Awh, E. (2017). Alpha-band activity reveals spontaneous representations of spatial position in visual working memory. *Current Biology*, *27*, 3216–3223. <https://doi.org/10.1016/j.cub.2017.09.031>, PubMed: 29033335
- Golomb, J. D., Chun, M. M., & Mazer, J. A. (2008). The native coordinate system of spatial attention is retinotopic. *Journal of Neuroscience*, *28*, 10654–10662. <https://doi.org/10.1523/JNEUROSCI.2525-08.2008>, PubMed: 18923041
- Gould, I. C., Rushworth, M. F., & Nobre, A. C. (2011). Indexing the graded allocation of visuospatial attention using anticipatory alpha oscillations. *Journal of Neurophysiology*, *105*, 1318–1326. <https://doi.org/10.1152/jn.00653.2010>, PubMed: 21228304
- Grent-'t-Jong, T., Boehler, C. N., Kenemans, J. L., & Woldorff, M. G. (2011). Differential functional roles of slow-wave and oscillatory-alpha activity in visual sensory cortex during anticipatory visual–spatial attention. *Cerebral Cortex*, *21*, 2204–2216. <https://doi.org/10.1093/cercor/bhq279>, PubMed: 21372123
- Gulbinaite, R., Roozendaal, D. H. M., & VanRullen, R. (2019). Attention differentially modulates the amplitude of resonance frequencies in the visual cortex. *Neuroimage*, *203*, 116146. <https://doi.org/10.1016/j.neuroimage.2019.116146>, PubMed: 31493535
- Gulbinaite, R., van Viegen, T., Wieling, M., Cohen, M. X., & VanRullen, R. (2017). Individual alpha peak frequency predicts 10 Hz flicker effects on selective attention. *Journal of Neuroscience*, *37*, 10173–10184. <https://doi.org/10.1523/JNEUROSCI.1163-17.2017>, PubMed: 28931569
- Harrison, S. A., & Tong, F. (2009). Decoding reveals the contents of visual working memory in early visual areas. *Nature*, *458*, 632–635. <https://doi.org/10.1038/nature07832>, PubMed: 19225460

- Ikkai, A., Dandekar, S., & Curtis, C. E. (2016). Lateralization in alpha-band oscillations predicts the locus and spatial distribution of attention. *PLoS One*, *11*, e0154796. <https://doi.org/10.1371/journal.pone.0154796>, PubMed: 27144717
- Kahneman, D., Treisman, A., & Gibbs, B. J. (1992). The reviewing of object files: Object-specific integration of information. *Cognitive Psychology*, *24*, 175–219. [https://doi.org/10.1016/0010-0285\(92\)90007-O](https://doi.org/10.1016/0010-0285(92)90007-O), PubMed: 1582172
- Kashiwase, Y., Matsumiya, K., Kuriki, I., & Shioiri, S. (2012). Time courses of attentional modulation in neural amplification and synchronization measured with steady-state visual-evoked potentials. *Journal of Cognitive Neuroscience*, *24*, 1779–1793. https://doi.org/10.1162/jocn_a_00212, PubMed: 22360591
- Keitel, C., Keitel, A., Benwell, C. S. Y., Daube, C., Thut, G., & Gross, J. (2019). Stimulus-driven brain rhythms within the alpha band: The attentional-modulation conundrum. *Journal of Neuroscience*, *39*, 3119–3129. <https://doi.org/10.1523/JNEUROSCI.1633-18.2019>, PubMed: 30770401
- Kelly, S. P., Gomez-Ramirez, M., & Foxe, J. J. (2009). The strength of anticipatory spatial biasing predicts target discrimination at attended locations: A high-density EEG study. *European Journal of Neuroscience*, *30*, 2224–2234. <https://doi.org/10.1111/j.1460-9568.2009.06980.x>, PubMed: 19930401
- Kleiner, M., Brainard, D., Pelli, D., Ingling, A., Murray, R., & Broussard, C. (2007). What's new in psychtoolbox-3. *Perception*, *36*, 1–16.
- Knight, J. B., Marsh, R. L., Brewer, G. A., & Clementz, B. A. (2012). Preparatory distributed cortical synchronization determines execution of some, but not all, future intentions. *Psychophysiology*, *49*, 1155–1167. <https://doi.org/10.1111/j.1469-8986.2012.01400.x>, PubMed: 22748058
- Kuo, B.-C., Rao, A., Lepsien, J., & Nobre, A. C. (2009). Searching for targets within the spatial layout of visual short-term memory. *Journal of Neuroscience*, *29*, 8032–8038. <https://doi.org/10.1523/JNEUROSCI.0952-09.2009>, PubMed: 19553443
- Kustov, A. A., & Lee Robinson, D. (1996). Shared neural control of attentional shifts and eye movements. *Nature*, *384*, 74–77. <https://doi.org/10.1038/384074a0>, PubMed: 8900281
- Liu, B., Nobre, A. C., & van Ede, F. (2022). Functional but not obligatory link between microsaccades and neural modulation by covert spatial attention. *Nature Communications*, *13*, 3503. <https://doi.org/10.1038/s41467-022-31217-3>, PubMed: 35715471
- Liu, B., Nobre, A. C., & van Ede, F. (2023). Microsaccades transiently lateralise EEG alpha activity. *Progress in Neurobiology*, *224*, 102433. <https://doi.org/10.1016/j.pneurobio.2023.102433>, PubMed: 36907349
- Logie, R. H., & Marchetti, C. (1991). Chapter 7. Visuo-spatial working memory: Visual, spatial or central executive? In R. H. Logie & M. Denis (Eds.), *Advances in psychology* (Vol. 80, pp. 105–115). North-Holland. [https://doi.org/10.1016/S0166-4115\(08\)60507-5](https://doi.org/10.1016/S0166-4115(08)60507-5)
- Maris, E., & Oostenveld, R. (2007). Nonparametric statistical testing of EEG- and MEG-data. *Journal of Neuroscience Methods*, *164*, 177–190. <https://doi.org/10.1016/j.jneumeth.2007.03.024>, PubMed: 17517438
- Minarik, T., Berger, B., & Jensen, O. (2023). Optimal parameters for rapid (invisible) frequency tagging using MEG. *Neuroimage*, *281*, 120389. <https://doi.org/10.1016/j.neuroimage.2023.120389>, PubMed: 37751812
- Morgan, S. T., Hansen, J. C., & Hillyard, S. A. (1996). Selective attention to stimulus location modulates the steady-state visual evoked potential. *Proceedings of the National Academy of Sciences, U.S.A.*, *93*, 4770–4774. <https://doi.org/10.1073/pnas.93.10.4770>, PubMed: 8643478
- Müller, M. M., Andersen, S., Trujillo, N. J., Valdés-Sosa, P., Malinowski, P., & Hillyard, S. A. (2006). Feature-selective attention enhances color signals in early visual areas of the human brain. *Proceedings of the National Academy of Sciences, U.S.A.*, *103*, 14250–14254. <https://doi.org/10.1073/pnas.0606668103>, PubMed: 16956975
- Müller, H. J., & Rabbitt, P. M. (1989). Reflexive and voluntary orienting of visual attention: Time course of activation and resistance to interruption. *Journal of Experimental Psychology: Human Perception and Performance*, *15*, 315–330. <https://doi.org/10.1037//0096-1523.15.2.315>, PubMed: 2525601
- Nobre, A. C., & van Ede, F. (2023). Attention in flux. *Neuron*, *111*, 971–986. <https://doi.org/10.1016/j.neuron.2023.02.032>, PubMed: 37023719
- Pan, Y., Frisson, S., & Jensen, O. (2021). Neural evidence for lexical parafoveal processing. *Nature Communications*, *12*, 5234. <https://doi.org/10.1038/s41467-021-25571-x>, PubMed: 34475391
- Perlstein, W. M., Cole, M. A., Larson, M., Kelly, K., Seignourel, P., & Keil, A. (2003). Steady-state visual evoked potentials reveal frontally-mediated working memory activity in humans. *Neuroscience Letters*, *342*, 191–195. [https://doi.org/10.1016/S0304-3940\(03\)00226-X](https://doi.org/10.1016/S0304-3940(03)00226-X), PubMed: 12757897
- Peters, B., Kaiser, J., Rahm, B., & Bledowski, C. (2021). Object-based attention prioritizes working memory contents at a theta rhythm. *Journal of Experimental Psychology: General*, *150*, 1250–1256. <https://doi.org/10.1037/xge0000994>, PubMed: 33211526
- Peterson, D. J., Gurariy, G., Dimotsantos, G. G., Arciniega, H., Berryhill, M. E., & Caplovitz, G. P. (2014). The steady-state visual evoked potential reveals neural correlates of the items encoded into visual working memory. *Neuropsychologia*, *63*, 145–153. <https://doi.org/10.1016/j.neuropsychologia.2014.08.020>, PubMed: 25173712
- Poch, C., Campo, P., & Barnes, G. R. (2014). Modulation of alpha and gamma oscillations related to retrospectively orienting attention within working memory. *European Journal of Neuroscience*, *40*, 2399–2405. <https://doi.org/10.1111/ejn.12589>, PubMed: 24750388
- Poch, C., Capilla, A., Hinojosa, J. A., & Campo, P. (2017). Selection within working memory based on a color retro-cue modulates alpha oscillations. *Neuropsychologia*, *106*, 133–137. <https://doi.org/10.1016/j.neuropsychologia.2017.09.027>, PubMed: 28958909
- Pomper, U., & Ansorge, U. (2021). Theta-rhythmic oscillation of working memory performance. *Psychological Science*, *32*, 1801–1810. <https://doi.org/10.1177/09567976211013045>, PubMed: 34592108
- Rademaker, R. L., Chunharas, C., & Serences, J. T. (2019). Coexisting representations of sensory and mnemonic information in human visual cortex. *Nature Neuroscience*, *22*, 1336–1344. <https://doi.org/10.1038/s41593-019-0428-x>, PubMed: 31263205
- Sauseng, P., Klimesch, W., Stadler, W., Schabus, M., Doppelmayr, M., Hanslmayr, S., et al. (2005). A shift of visual spatial attention is selectively associated with human EEG alpha activity. *European Journal of Neuroscience*, *22*, 2917–2926. <https://doi.org/10.1111/j.1460-9568.2005.04482.x>, PubMed: 16324126
- Schall, J. D., & Hanes, D. P. (1993). Neural basis of saccade target selection in frontal eye field during visual search. *Nature*, *366*, 467–469. <https://doi.org/10.1038/366467a0>, PubMed: 8247155
- Schneegans, S., & Bays, P. M. (2017). Neural architecture for feature binding in visual working memory. *Journal of Neuroscience*, *37*, 3913–3925. <https://doi.org/10.1523/JNEUROSCI.3493-16.2017>, PubMed: 28270569

- Schneider, Z., Parker, D., Kittle, F., McDowell, J., Buckley, P., Keedy, S., et al. (2017). SU5. Investigation of the visual steady-state response in schizophrenia, schizoaffective, psychotic, and nonpsychotic bipolar disorders. *Schizophrenia Bulletin*, *43*(Suppl. 1), S162. <https://doi.org/10.1093/schbul/sbx024.004>
- Serences, J. T., Ester, E. F., Vogel, E. K., & Awh, E. (2009). Stimulus-specific delay activity in human primary visual cortex. *Psychological Science*, *20*, 207–214. <https://doi.org/10.1111/j.1467-9280.2009.02276.x>, PubMed: 19170936
- Siegel, M., Donner, T. H., Oostenveld, R., Fries, P., & Engel, A. K. (2008). Neuronal synchronization along the dorsal visual pathway reflects the focus of spatial attention. *Neuron*, *60*, 709–719. <https://doi.org/10.1016/j.neuron.2008.09.010>, PubMed: 19038226
- Silberstein, R. B., Nunez, P. L., Pipingas, A., Harris, P., & Danieli, F. (2001). Steady state visually evoked potential (SSVEP) topography in a graded working memory task. *International Journal of Psychophysiology*, *42*, 219–232. [https://doi.org/10.1016/S0167-8760\(01\)00167-2](https://doi.org/10.1016/S0167-8760(01)00167-2), PubMed: 11587778
- Smyth, M. M. (1996). Interference with rehearsal in spatial working memory in the absence of eye movements. *Quarterly Journal of Experimental Psychology: A, Human Experimental Psychology*, *49*, 940–949. <https://doi.org/10.1080/713755669>, PubMed: 8962542
- Souza, A. S., & Oberauer, K. (2016). In search of the focus of attention in working memory: 13 years of the retro-cue effect. *Attention, Perception, & Psychophysics*, *78*, 1839–1860. <https://doi.org/10.3758/s13414-016-1108-5>, PubMed: 27098647
- Theeuwes, J., Kramer, A. F., & Irwin, D. E. (2011). Attention on our mind: The role of spatial attention in visual working memory. *Acta Psychologica*, *137*, 248–251. <https://doi.org/10.1016/j.actpsy.2010.06.011>, PubMed: 20637448
- Thigpen, N., Petro, N. M., Oschwald, J., Oberauer, K., & Keil, A. (2019). Selection of visual objects in perception and working memory one at a time. *Psychological Science*, *30*, 1259–1272. <https://doi.org/10.1177/0956797619854067>, PubMed: 31322983
- Thut, G., Nietzel, A., Brandt, S. A., & Pascual-Leone, A. (2006). α -Band electroencephalographic activity over occipital cortex indexes visuospatial attention bias and predicts visual target detection. *Journal of Neuroscience*, *26*, 9494–9502. <https://doi.org/10.1523/JNEUROSCI.0875-06.2006>, PubMed: 16971533
- Toffanin, P., de Jong, R., Johnson, A., & Martens, S. (2009). Using frequency tagging to quantify attentional deployment in a visual divided attention task. *International Journal of Psychophysiology*, *72*, 289–298. <https://doi.org/10.1016/j.ijpsycho.2009.01.006>, PubMed: 19452603
- Treisman, A. (1988). Features and objects: The fourteenth Bartlett memorial lecture. *Quarterly Journal of Experimental Psychology: A, Human Experimental Psychology*, *40*, 201–237. <https://doi.org/10.1080/02724988843000104>, PubMed: 3406448
- van Ede, F., Board, A. G., & Nobre, A. C. (2020). Goal-directed and stimulus-driven selection of internal representations. *Proceedings of the National Academy of Sciences, U.S.A.*, *117*, 24590–24598. <https://doi.org/10.1073/pnas.2013432117>, PubMed: 32929036
- van Ede, F., Chekroud, S. R., & Nobre, A. C. (2019). Human gaze tracks attentional focusing in memorized visual space. *Nature Human Behaviour*, *3*, 462–470. <https://doi.org/10.1038/s41562-019-0549-y>, PubMed: 31089296
- van Ede, F., Deden, J., & Nobre, A. C. (2021). Looking ahead in working memory to guide sequential behaviour. *Current Biology*, *31*, R779–R780. <https://doi.org/10.1016/j.cub.2021.04.063>, PubMed: 34157258
- van Ede, F., Niklaus, M., & Nobre, A. C. (2017). Temporal expectations guide dynamic prioritization in visual working memory through attenuated α oscillations. *Journal of Neuroscience*, *37*, 437–445. <https://doi.org/10.1523/JNEUROSCI.2272-16.2016>, PubMed: 28077721
- Vissers, M. E., Gulbinaite, R., van den Bos, T., & Slagter, H. A. (2017). Protecting visual short-term memory during maintenance: Attentional modulation of target and distractor representations. *Scientific Reports*, *7*, 4061. <https://doi.org/10.1038/s41598-017-03995-0>, PubMed: 28642613
- Vogel, E. K., McCollough, A. W., & Machizawa, M. G. (2005). Neural measures reveal individual differences in controlling access to working memory. *Nature*, *438*, 500–503. <https://doi.org/10.1038/nature04171>, PubMed: 16306992
- Walter, S., Quigley, C., Andersen, S. K., & Mueller, M. M. (2012). Effects of overt and covert attention on the steady-state visual evoked potential. *Neuroscience Letters*, *519*, 37–41. <https://doi.org/10.1016/j.neulet.2012.05.011>, PubMed: 22579858
- Wang, J., Clementz, B. A., & Keil, A. (2007). The neural correlates of feature-based selective attention when viewing spatially and temporally overlapping images. *Neuropsychologia*, *45*, 1393–1399. <https://doi.org/10.1016/j.neuropsychologia.2006.10.019>, PubMed: 17161441
- Willet, S. M., & Mayo, J. P. (2023). Microsaccades are directed toward the midpoint between targets in a variably cued attention task. *Proceedings of the National Academy of Sciences, U.S.A.*, *120*, e2220552120. <https://doi.org/10.1073/pnas.2220552120>, PubMed: 37155892
- Wu, Z., Yao, D., Tang, Y., Huang, Y., & Su, S. (2010). Amplitude modulation of steady-state visual evoked potentials by event-related potentials in a working memory task. *Journal of Biological Physics*, *36*, 261–271. <https://doi.org/10.1007/s10867-009-9181-9>, PubMed: 19960240
- Yang, H., Paller, K. A., & van Vugt, M. (2022). The steady state visual evoked potential (SSVEP) tracks “sticky” thinking, but not more general mind-wandering. *Frontiers in Human Neuroscience*, *16*, 892863. <https://doi.org/10.3389/fnhum.2022.892863>, PubMed: 36034124
- Zhigalov, A., & Jensen, O. (2020). Alpha oscillations do not implement gain control in early visual cortex but rather gating in parieto-occipital regions. *Human Brain Mapping*, *41*, 5176–5186. <https://doi.org/10.1002/hbm.25183>, PubMed: 32822098
- Zhou, H., & Desimone, R. (2011). Feature-based attention in the frontal eye field and area V4 during visual search. *Neuron*, *70*, 1205–1217. <https://doi.org/10.1016/j.neuron.2011.04.032>, PubMed: 21689605